Cancer Cell, Volume *38*

Supplemental Information

Tumor Microenvironment-Derived NRG1 Promotes Antiandrogen Resistance in Prostate Cancer

Zeda Zhang, Wouter R. Karthaus, Young Sun Lee, Vianne R. Gao, Chao Wu, Joshua W. Russo, Menghan Liu, Jose Mauricio Mota, Wassim Abida, Eliot Linton, Eugine Lee, Spencer D. Barnes, Hsuan-An Chen, Ninghui Mao, John Wongvipat, Danielle Choi, Xiaoping Chen, Huiyong Zhao, Katia Manova-Todorova, Elisa de Stanchina, Mary-Ellen Taplin, Steven P. Balk, Dana E. Rathkopf, Anuradha Gopalan, Brett S. Carver, Ping Mu, Xuejun Jiang, Philip A. Watson, and Charles L. Sawyers

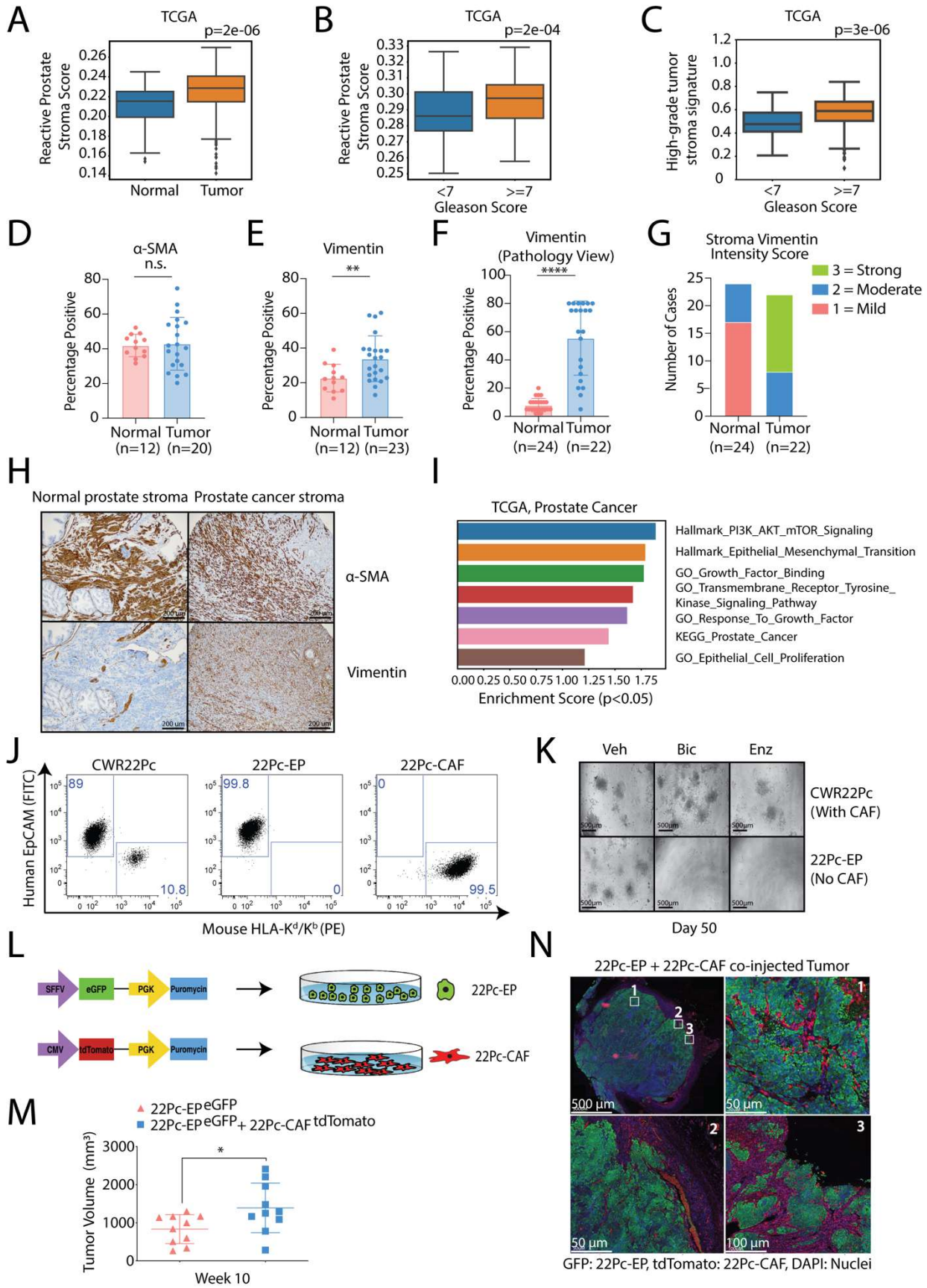
A
TCGA
p=2e-06
Reactive Prostate Stroma Score
Normal
Tumor
B
TCGA
p=2e-04
Reactive Prostate Stroma Score
<7
>=7
Gleason Score
C
TCGA
p=3e-06
High-grade tumor stroma signature
<7
>=7
Gleason Score
D
α-SMA
n.s.
Percentage Positive
Normal (n=12)
Tumor (n=20)
E
Vimentin
**
Percentage Positive
Normal (n=12)
Tumor (n=23)
F
Vimentin (Pathology View)
****
Percentage Positivie
Normal (n=24)
Tumor (n=22)
G
Stroma Vimentin Intensity Score
3 = Strong
2 = Moderate
1 = Mild
Number of Cases
Normal (n=24)
Tumor (n=22)
H
Normal prostate stroma
Prostate cancer stroma
α-SMA
Vimentin
200 um
I
TCGA, Prostate Cancer
Hallmark_PI3K_AKT_mTOR_Signaling
Hallmark_Epithelial_Mesenchymal_Transition
GO_Growth_Factor_Binding
GO_Transmembrane_Receptor_Tyrosine_Kinase_Signaling_Pathway
GO_Response_To_Growth_Factor
KEGG_Prostate_Cancer
GO_Epithelial_Cell_Proliferation
0.00 0.25 0.50 0.75 1.00 1.25 1.50 1.75
Enrichment Score (p<0.05)
J
CWR22Pc
22Pc-EP
22Pc-CAF
89
10.8
99.8
0
0
99.5
Human EpCAM (FITC)
Mouse HLA-Kd/Kb (PE)
K
Veh
Bic
Enz
CWR22Pc (With CAF)
22Pc-EP (No CAF)
500μm
Day 50
L
SFFV
eGFP
PGK
Puromycin
CMV
tdTomato
22Pc-EP
22Pc-CAF
M
22Pc-EP eGFP
22Pc-EP eGFP + 22Pc-CAF tdTomato
Tumor Volume (mm3)
*
Week 10
N
22Pc-EP + 22Pc-CAF co-injected Tumor
1
2
3
500 μm
50 μm
100 μm
GFP: 22Pc-EP, tdTomato: 22Pc-CAF, DAPI: Nuclei

Figure S1 related to Figure 1. Cancer-associated fibroblasts (CAF) promote antiandrogen resistance in an androgen dependent PCa model.

(A) Comparison of reactive prostate stroma score between normal prostate tissue and primary prostate cancer tissue in TCGA cohort, p value=$2x10^{-6}$. See details in STAR methods.

(B) Comparison of reactive prostate stroma score between tumors with Gleason score <7 and those >=7, p value=$2x10^{-4}$. See details in STAR methods.

(C) Comparison of high-grade tumor associated stroma signature score between tumors with Gleason score <7 and those >=7, p value=$3x10^{-6}$. See details in methods.

(D-E) Quantification of immunohistochemistry analysis of α-SMA (D) or vimentin (E) in the prostate tissue array using ImageJ IHC profiler plugin (**p<0.01, Student's t-test, data are represented as mean±SD).

(F) Quantification of stroma-specific vimentin intensity in the prostate cancer tissue microarray. ****p<0.0001, Student's t-test, data are represented as mean±SD.

(G) Histogram showing distribution of vimentin intensity case numbers in the prostate cancer tissue microarray (1=mild, 2=moderate and 3=strong).

(H) Immunohistochemistry analysis of α-SMA and vimentin in normal prostate gland and prostate cancer specimens in the prostate cancer tissue microarray.

(I) Pathway enrichment analysis showing top-ranking enriched pathways between tumors with high reactive stroma activity versus those with low reactive stroma activity in TCGA cohort (p value<0.05, FDR<0.25).

(J) Isolation of 22Pc-EP and 22Pc-CAF by FACS using human-specific EpCAM and mouse-specific H-$2K^b$/H-$2D^b$ MHC class I surface marker staining.

(K) Representative images showing results of colony formation assay of CWR22Pc and 22Pc-EP cells treated with Veh (DMSO), Bic (10 μM) or Enz (0.1 μM) on day 50.

(L) Schematic diagram of the generation of 22c-EP^{eGFP} and 22Pc-$CAF^{tdTomato}$ by viral transduction.

(M) Tumor volumes of 22Pc-EP^{eGFP} or co-injected 22Pc-EP^{eGFP} + 22Pc-$CAF^{tdTomato}$ xenografts at week 10 (n=5 mice per group, *p<0.05, Student's t-test, data are represented as mean±SEM).

(N) Immunofluorescence analysis of tumor infiltrating 22Pc-$CAF^{tdTomato}$ cells in 22c-EP^{eGFP} + 22Pc-$CAF^{tdTomato}$ co-injected xenografts at week 10 (Green: 22c-EP^{eGFP}, Red: 22Pc-$CAF^{tdTomato}$).

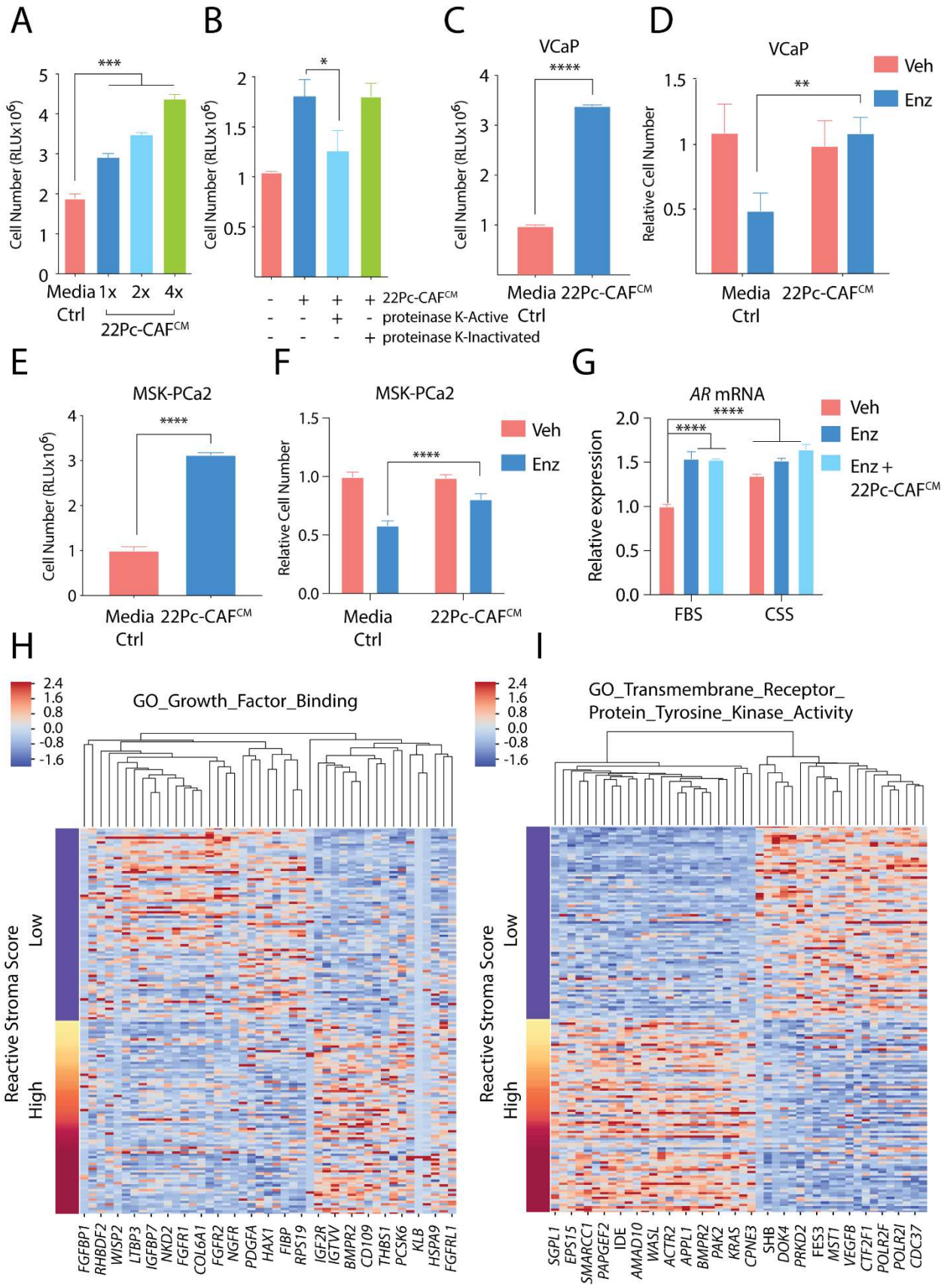
A
B
C
D
Cell Number (RLUx10^6)
***
Media Ctrl
1x
2x
4x
22Pc-CAF^CM
*
- + + + 22Pc-CAF^CM
- - + - proteinase K-Active
- - - + proteinase K-Inactivated
VCaP
****
Media Ctrl
22Pc-CAF^CM
Relative Cell Number
**
Veh
Enz
E
F
G
MSK-PCa2
Relative expression
AR mRNA
Enz + 22Pc-CAF^CM
FBS
CSS
H
I
GO_Growth_Factor_Binding
GO_Transmembrane_Receptor_ Protein_Tyrosine_Kinase_Activity
Reactive Stroma Score
Low
High
FGFBP1 RHBDF2 WISP2 LTBP3 IGFBP7 NKD2 FGFR1 COL6A1 FGFR2 NGFR PDGFA HAX1 FIBP RPS19 IGF2R IGTV BMPR2 CD109 THBS1 PCSK6 KLB HSPA9 FGFRL1
SGPL1 EPS15 SMARCC1 PAPGEF2 IDE AMAD10 WASL ACTR2 APPL1 BMPR2 PAK2 KRAS CPNE3 SHB DOK4 PRKD2 FES3 MST1 VEGFB CTF2F1 POLR2F POLR2I CDC37

Figure S2 related to Figure 2. CAF-secreted factors promote antiandrogen resistance.
(A) Growth of 22Pc-EP cells in CSS media supplemented with increasing concentration of 22Pc-CAF^{CM} (1x, 2x and 4x). CellTiter-Glo reading on day 4. Media Ctrl: serum free media.
(B) Growth of 22Pc-EP cells in CSS media supplemented with 22Pc-CAF^{CM} treated with proteinase K (200µg/mL) or heat-inactivated proteinase K. CellTiter-Glo reading on day 4. Media Ctrl: serum free media.
(C) Growth of VCaP cells in CSS media supplemented with 22Pc-CAF^{CM}. CellTiter-Glo reading on day 4. Media Ctrl: serum free media.
(D) Growth of VCaP cells in Enz (1 µM) or Veh (DMSO) containing FBS media supplemented with 22Pc-CAF^{CM}. CellTiter-Glo reading on day 7. Media Ctrl: serum free media.
(E) Growth of patient-derived cancer organoid MSK-PCa2 in DHT-deficient organoid media supplemented with 22Pc-CAF^{CM}. CellTiter-Glo reading on day 4. Media Ctrl: EGF-deficient organoid media.
(F) Growth of patient-derived cancer organoid MSK-PCa2 in Enz (1 µM) or Veh (DMSO) containing human organoid media supplemented with 22Pc-CAF^{CM}. CellTiter-Glo reading on day 7. Media Ctrl: EGF-deficient organoid media.
(G) qRT-PCR analysis of *AR* mRNA expression in 22Pc-EP cells treated with Enz, 22Pc-CAF^{CM} or Enz + 22Pc-CAF^{CM} for 24 h. *AR* expression was normalized to *ACTB*.
(H) Heatmap showing unsupervised clustering with Growth Factor Binding gene signature between tumors with high reactive stroma score and tumors with low score (TCGA). See details in STAR methods.
(I) Heatmap showing unsupervised clustering using Transmembrane Receptor Protein Tyrosine Kinase Activity signature between tumors with high reactive stroma score and tumors with low score (TCGA). See details in STAR methods.

Assays were performed with three biological replicates. ****p<0.0001, ***p<0.001, **p<0.01, *p<0.05, n.s.: not significant, A,G: one-way ANOVA, B-F: Student's t-test. Data are represented as mean±SD)

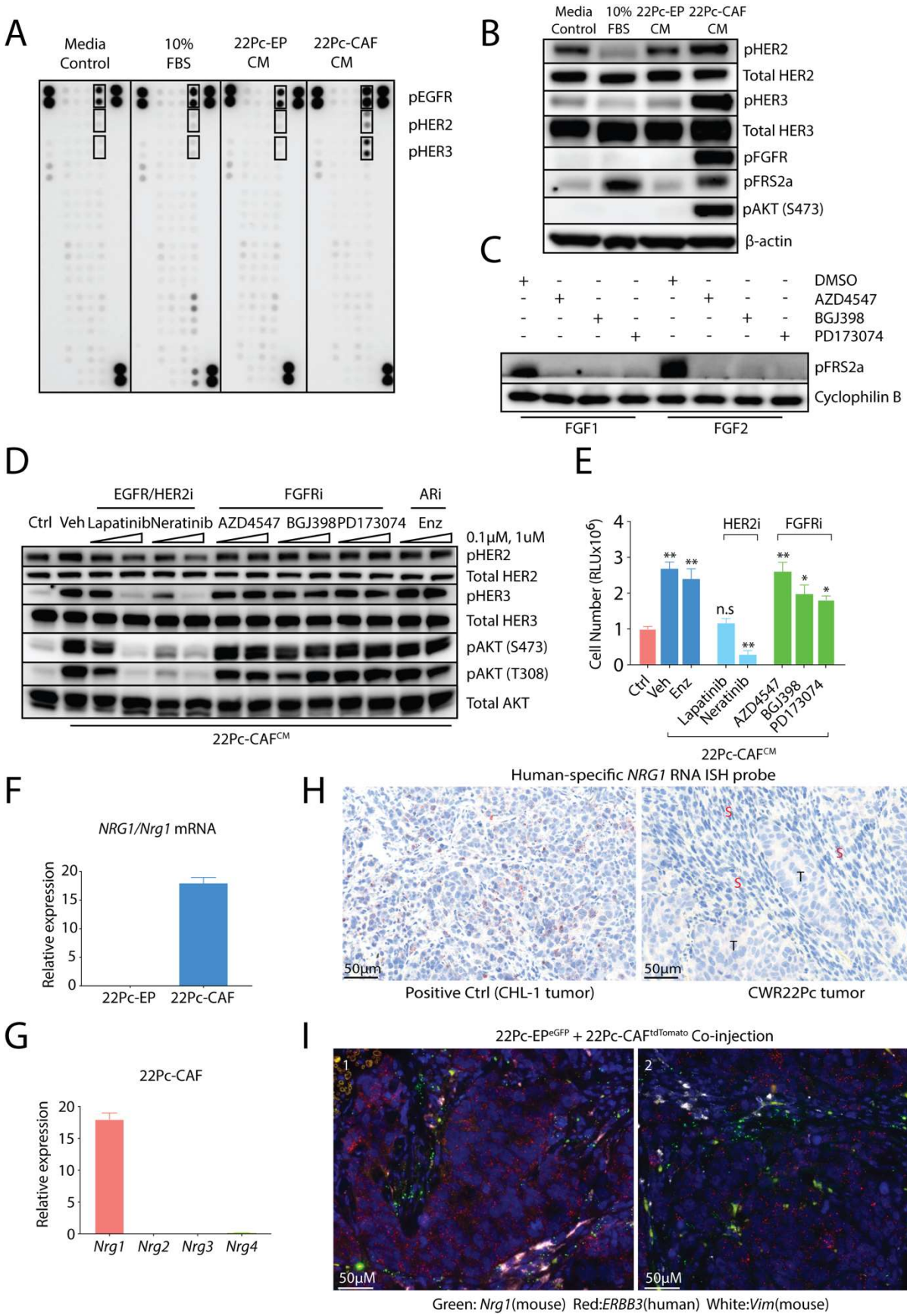
A
Media Control
10% FBS
22Pc-EP CM
22Pc-CAF CM
pEGFR
pHER2
pHER3
B
Media Control
10% FBS
22Pc-EP CM
22Pc-CAF CM
pHER2
Total HER2
pHER3
Total HER3
pFGFR
pFRS2a
pAKT (S473)
β-actin
C
DMSO
AZD4547
BGJ398
PD173074
pFRS2a
Cyclophilin B
FGF1
FGF2
D
EGFR/HER2i
FGFRi
ARi
Ctrl
Veh
Lapatinib
Neratinib
AZD4547
BGJ398
PD173074
Enz
0.1μM, 1uM
pHER2
Total HER2
pHER3
Total HER3
pAKT (S473)
pAKT (T308)
Total AKT
22Pc-CAF^CM
E
Cell Number (RLUx10^6)
HER2i
FGFRi
n.s
Ctrl
Veh
Enz
Lapatinib
Neratinib
AZD4547
BGJ398
PD173074
22Pc-CAF^CM
F
NRG1/Nrg1 mRNA
Relative expression
22Pc-EP
22Pc-CAF
G
22Pc-CAF
Relative expression
Nrg1
Nrg2
Nrg3
Nrg4
H
Human-specific NRG1 RNA ISH probe
S
T
50μm
Positive Ctrl (CHL-1 tumor)
CWR22Pc tumor
I
22Pc-EP^eGFP + 22Pc-CAF^tdTomato Co-injection
1
2
50μM
Green: Nrg1(mouse) Red:ERBB3(human) White:Vim(mouse)

Figure S3 related to Figure 3. Biochemical fractionation of CAF-secreted resistance activity implicates neuregulin 1.

(A) Human Receptor Tyrosine Kinase (RTK) array analysis of serum starved 22Pc-EP after stimulation with either 10% FBS media, 22Pc-EP^{CM} or 22Pc-CAF^{CM} or serum free media control.

(B) Western blot analysis of HER2/3-AKT activation in 22Pc-EP cell lysates from S3A. β-actin serves as loading control.

(C) Western blot analysis of FGFR activation (pFRS2a) in 22Pc-EP cells after stimulation with FGF1 or FGF2 (50 ng/mL) in the presence of different FGFR inhibitors (AZD4547, BGJ398 or PD173074, each at 1 μM) or Veh (DMSO). Cyclophilin B serves as loading control.

(D) Western blot analysis of HER3-PI3K activation in 22Pc-EP cells after stimulation with 22Pc-CAF^{CM} in the presence of inhibitors of either AR (Enz: 0.1 μM, 1 μM), HER2 (lapatinib: 0.1 μM, 1 μM or neratinib: 0.1 μM, 1 μM), FGFR (AZD4547, BGJ398, PD173074; each at 0.1 μM, 1 μM) or Veh (DMSO). Total AKT serves as loading control. Ctrl: serum free media.

(E) Growth of 22Pc-EP cells in CSS media supplemented with 22Pc-CAF^{CM} in the presence of HER2 inhibitors (lapatinib: 1 μM or neratinib: 0.1 μM), FGFR inhibitors (AZD4547, BGJ398, PD173074, each at 1 μM) or Veh (DMSO). CellTiter-Glo reading on day 4. Ctrl: serum free media (Assays were performed with biological replicates. **p<0.01, *p<0.05, n.s.: not significant, one-way ANOVA, data are represented as mean±SD).

(F) qRT-PCR analysis of *NRG1/Nrg1* expression in 22Pc-EP or 22Pc-CAF using species-specific primers with three biological replicates. *NRG1/Nrg1* expression was normalized to *ACTB*/*Actb*.

(G) qRT-PCR analysis of different *Nrg1* family member expressions in 22Pc-CAF with three biological replicates. *Nrg1* expression was normalized to *Actb*.

(H) Representative images showing RNA *in situ* hybridization (ISH) analysis of human *NRG1* expression in CWR22Pc tumor xenografts. An *NRG1* positive human melanoma tumor xenograft (CHL-1) was used as a positive control (T: tumor, S: stroma, human specific *NRG1* probe: red dots).

(I) Representative images showing RNA-FISH analysis of *Nrg1* expression in two independent CWR22Pc tumor xenografts (Green: mouse-*Nrg1*, Red: human-*ERBB3*, White: mouse-*Vim* and Blue: DAPI).

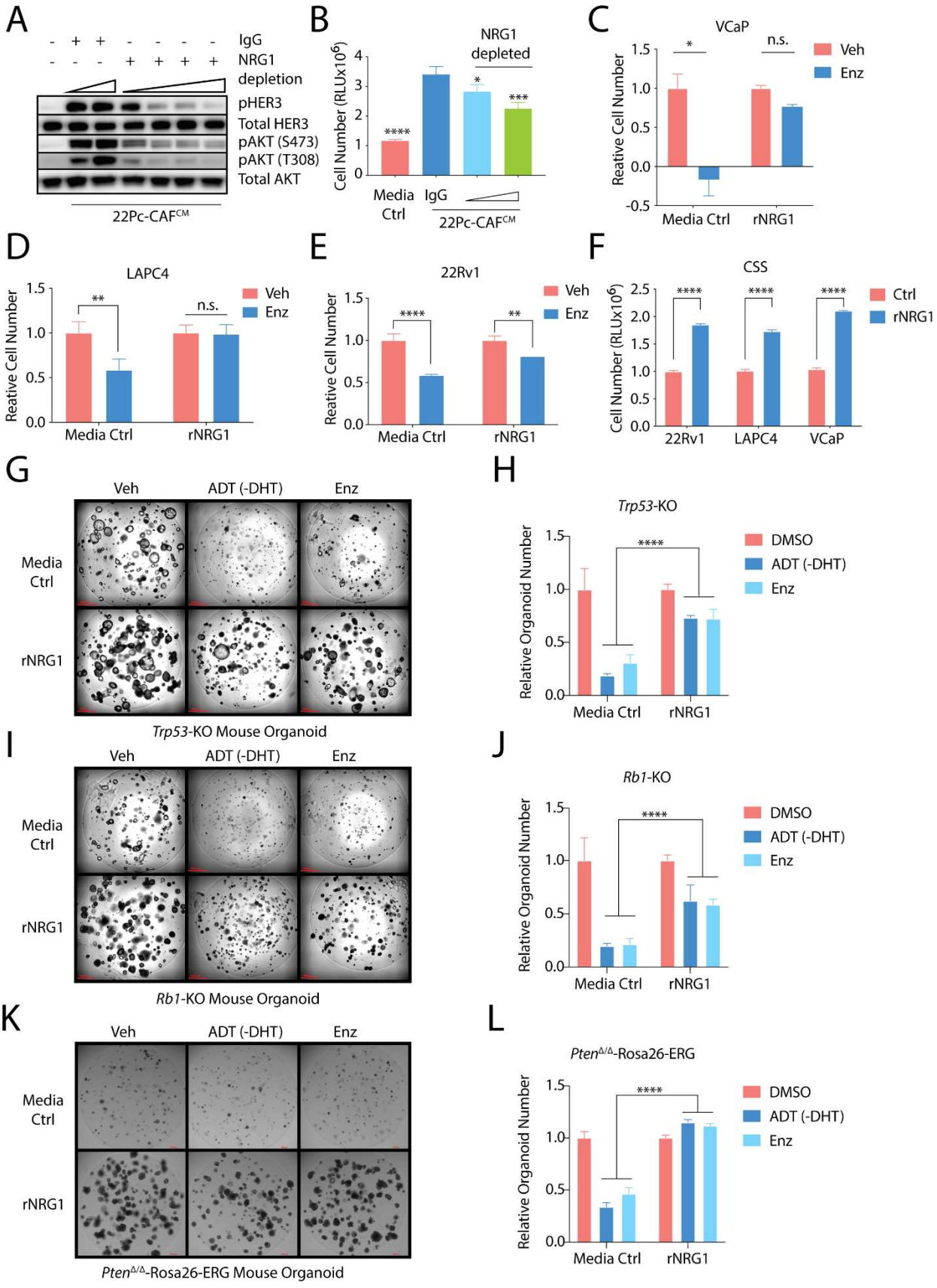
A
IgG
NRG1 depletion
pHER3
Total HER3
pAKT (S473)
pAKT (T308)
Total AKT
22Pc-CAF^CM
B
NRG1 depleted
Cell Number (RLUx10^6)
Media Ctrl
IgG
22Pc-CAF^CM
C
VCaP
Reative Cell Number
Veh
Enz
Media Ctrl
rNRG1
D
LAPC4
E
22Rv1
F
CSS
Ctrl
rNRG1
22Rv1
LAPC4
VCaP
G
Veh
ADT (-DHT)
Enz
Media Ctrl
rNRG1
Trp53-KO Mouse Organoid
H
Trp53-KO
Relative Organoid Number
DMSO
ADT (-DHT)
Enz
I
Rb1-KO Mouse Organoid
J
Rb1-KO
K
Pten^Δ/Δ-Rosa26-ERG Mouse Organoid
L
Pten^Δ/Δ-Rosa26-ERG

Figure S4 related to Figure 4. NRG1 promotes antiandrogen resistance in androgen dependent PCa models.

(A) Western blot analysis of HER3-AKT activation in 22Pc-EP after stimulation with 22Pc-CAF^{CM} where NRG1 was depleted by immunoprecipitation using a commercial NRG1 antibody (1,10, 30 and 100μg/mL) or IgG (100μg/mL). Total AKT serves as loading control.

(B) Growth of 22Pc-EP cells in CSS media supplemented with NRG1-immunodepleted 22Pc-CAF^{CM} by a NRG1 immunoprecipitation antibody (10, 30μg/mL). CellTiter-Glo reading on day 4. Media Ctrl: serum free media.

(C) Growth of VCaP cells in Veh (DMSO) or Enz (1 μM) containing FBS media supplemented with recombinant NRG1 (10 ng/mL). CellTiter-Glo reading on day 7. Enz group is normalized to Veh group. Media Ctrl: serum free media.

(D) Growth of LAPC4 cells in Veh (DMSO)/FBS media or Enz (10 μM)/CSS media supplemented with recombinant NRG1 (10 ng/mL). CellTiter-Glo reading on day 7. Enz group is normalized to Veh group. Media Ctrl: serum free media.

(E) Growth of 22Rv1 cells in Veh (DMSO)/FBS media or Enz (10 μM)/CSS media supplemented with recombinant NRG1 (10 ng/mL). CellTiter-Glo reading on day 7. Enz group is normalized to Veh group. Media Ctrl: serum free media.

(F) Growth of 22Rv1, LAPC4 or VCaP cells in CSS media supplemented with recombinant NRG1 (10 ng/mL). CellTiter-Glo reading on day 4. Ctrl: serum free media.

(G) Representative images showing *Trp53*-KO mouse organoids in 3D culture supplemented with recombinant NRG1 and were treated with DHT depletion (ADT), Enz (1 μM) or Veh (DMSO). Images are taken on day 7.

(H) Growth of *Trp53*-KO mouse organoids in 3D culture supplemented with recombinant NRG1 (10 ng/mL) and were treated with ADT, Enz (1 μM) or Veh (DMSO). CellTiter-Glo reading on day 7. ADT or Enz was normalized to DMSO group. Ctrl: EGF-deficient organoid media.

(I) Representative images showing *Rb1*-KO mouse organoids in 3D culture supplemented with recombinant NRG1 and were treated with ADT, Enz (1 μM) or Veh (DMSO). Images were taken on day 7.

(J) Growth of *Rb1*-KO mouse organoids in 3D culture supplemented with recombinant NRG1 (10 ng/mL) and were treated with ADT or Enz (1 μM) or Veh (DMSO). CellTiter-Glo reading on day 7. ADT or Enz was normalized to DMSO group. Ctrl: EGF-deficient organoid media.

(K) Representative images showing *Pten*$^{\Delta/\Delta}$-Rosa26-ERG mouse organoids in 3D culture supplemented with recombinant NRG1 and were treated with ADT, Enz (1 μM) or Veh (DMSO). Images were taken on day 7.

(L) Growth of *Pten*$^{\Delta/\Delta}$-Rosa26-ERG mouse organoids in 3D culture supplemented with recombinant NRG1 (10 ng/mL) and were treated with ADT or Enz (1 μM) or Veh (DMSO). CellTiter-Glo reading on day 7. ADT or Enz was normalized to DMSO group. Ctrl: EGF-deficient organoid media.

Assays were performed with three biological replicates. ****p<0.0001, ***p<0.001, *p<0.05, n.s.: not significant, C-F, Student's t-test, H,J,L: one-way ANOVA compared to Ctrl group. Data are represented as mean±SD.

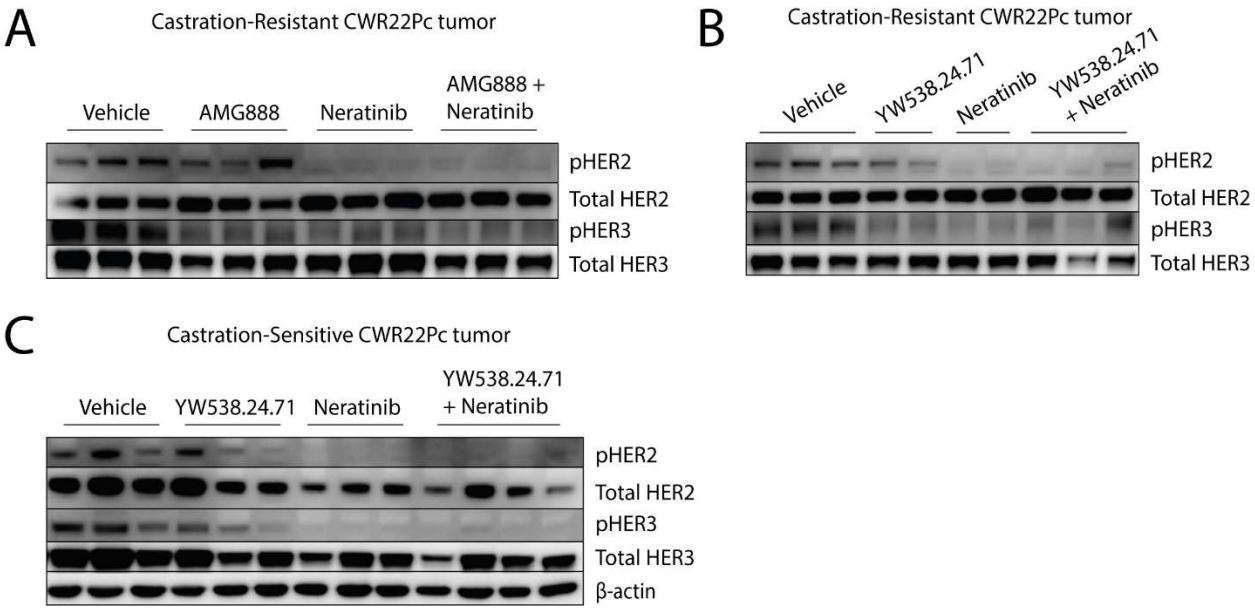

Figure S5 related to Figure 5. NRG1-HER3 signaling confers antiandrogen resistance *in vivo.*

(A) Western blot analysis of HER2/HER3 activation in castration-resistant CWR22Pc tumors treated with AMG888 (20 mg/kg), neratinib (20 mg/kg) or vehicle (DMSO). Total HER3 serves as loading control.

(B) Western blot analysis of HER2/HER3 activation in castration-resistant CWR22Pc tumors treated with YW538.24.71 (25 mg/kg), neratinib (20 mg/kg) or vehicle (DMSO). Total HER3 serves as loading control.

(C) Western blot analysis of HER2/HER2 activation in castration sensitive CWR22Pc tumors treated with castration plus AMG888 (20 mg/kg), neratinib (20 mg/kg) or vehicle (DMSO). β-actin serves as loading control.

#Note: For A-C, white “ghost-like” bands denote artifact due to longer time exposure with the hypersensitive ECL solution (Millipore # WBKLS0500) and do not affect the data interpretation.

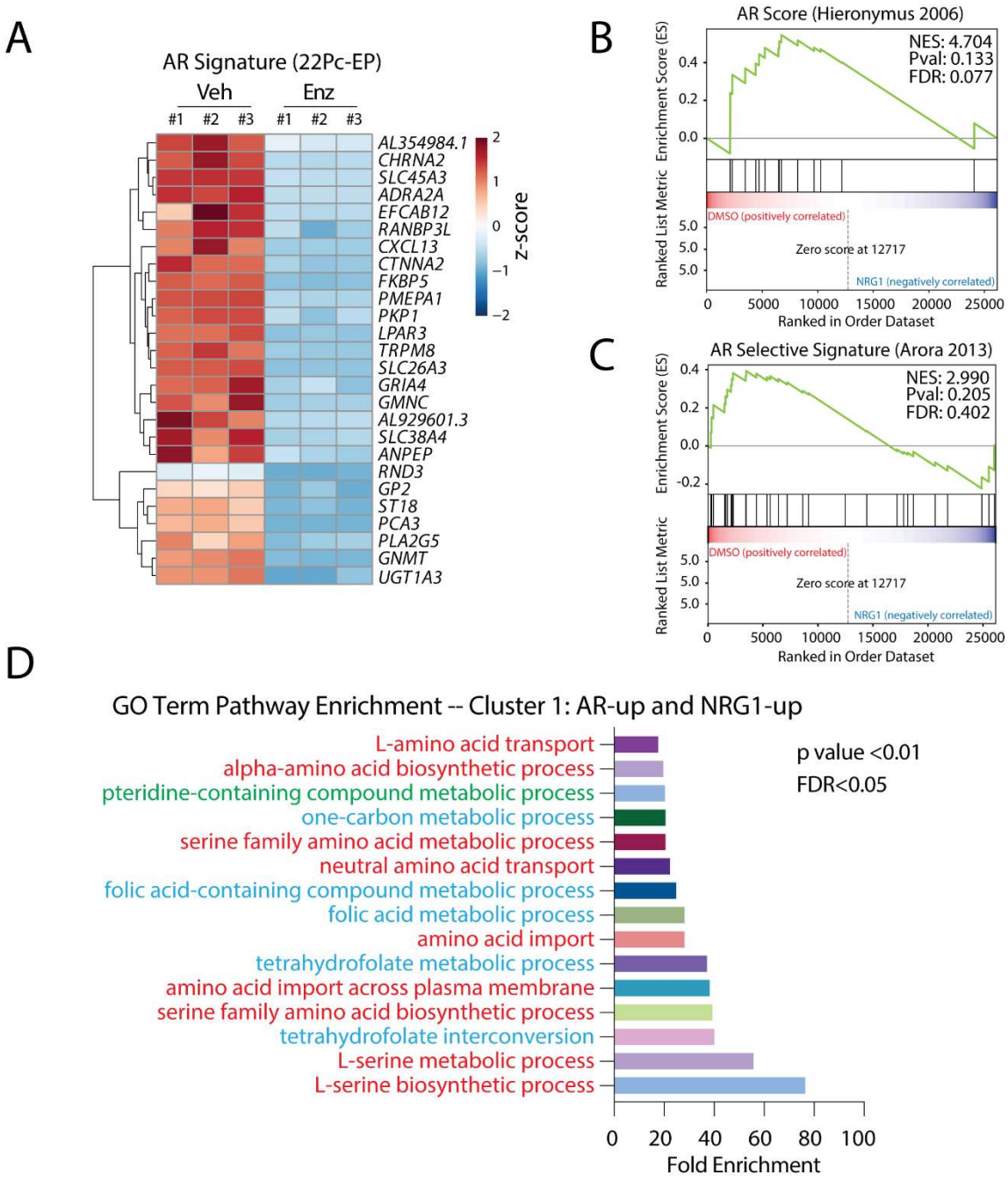

Figure S6 related to Figure 6. NRG1 activates a subset of AR target genes.
(A) Heatmap showing expression of individual genes (n=26) that consists of the AR signature in 22Pc-EP. AR signature genes were identified as Enz suppressed genes by comparing vehicle (Veh) to Enz condition (adjusted p value<0.05, log2 fold change>2).
(B) GSEA of AR score (Hieronymus et al., 2006) between DMSO versus NRG1-treated group in 22Pc-EP cells.
(C) GSEA of AR selective signature (Arora et al., 2013) between DMSO versus NRG1-treated group in 22Pc-EP cells.
(D) GO term analysis of top enriched pathways in cluster 1 (n=103 genes as input list, adjusted p value<0.05, log2 fold change>0.5).

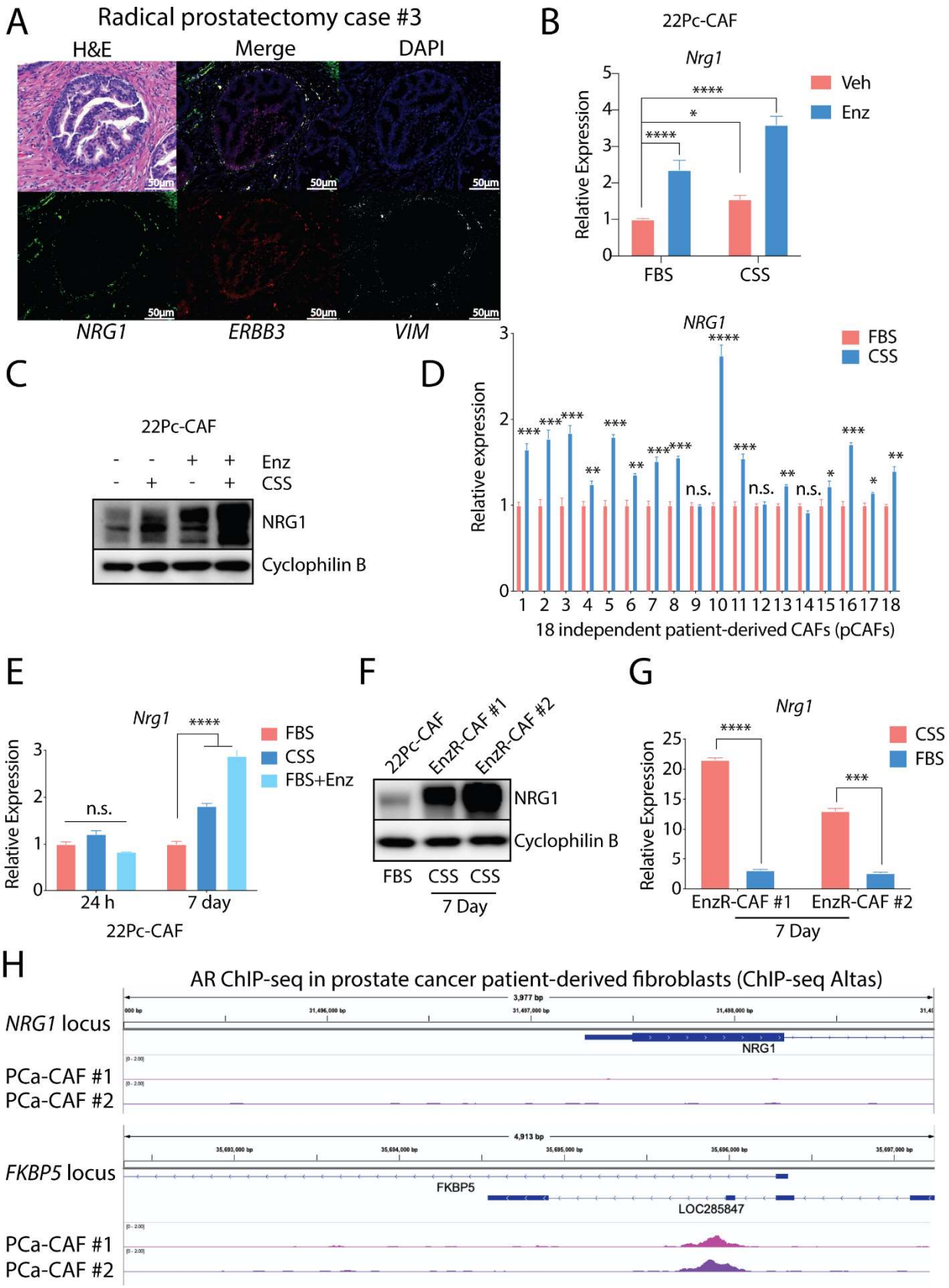
A
Radical prostatectomy case #3
H&E
Merge
DAPI
50µm
NRG1
ERBB3
VIM
B
22Pc-CAF
Nrg1
Relative Expression
Veh
Enz
****
*
FBS
CSS
C
22Pc-CAF
Enz
CSS
NRG1
Cyclophilin B
D
NRG1
FBS
CSS
Relative expression
18 independent patient-derived CAFs (pCAFs)
n.s.
E
Nrg1
FBS
CSS
FBS+Enz
Relative Expression
24 h
7 day
22Pc-CAF
F
22Pc-CAF
EnzR-CAF #1
EnzR-CAF #2
NRG1
Cyclophilin B
FBS
CSS
CSS
7 Day
G
Nrg1
CSS
FBS
Relative Expression
EnzR-CAF #1
EnzR-CAF #2
7 Day
H
AR ChIP-seq in prostate cancer patient-derived fibroblasts (ChIP-seq Altas)
NRG1 locus
PCa-CAF #1
PCa-CAF #2
FKBP5 locus
FKBP5
LOC285847

Figure S7 related to Figure 7. Androgen deprivation therapy induces NRG1 expression in the stroma of prostate cancer patients.
(A) RNA-FISH analysis of *NRG1* (green), *ERBB3* (red) and *VIM* (white) expression in a high-grade prostate intraductal carcinoma case (Blue: DAPI).
(B) qRT-PCR analysis of *Nrg1* mRNA expression in 22Pc-CAF treated with CSS, Enz (10 μM) or Veh (DMSO). *Nrg1* expression is normalized to *Actb*.
(C) Western blot analysis of NRG1 protein in 22Pc-CAF treated with CSS, Enz (10 μM) or Veh (DMSO). Cyclophilin B serves as loading control.
(D) qRT-PCR analysis of *NRG1* mRNA expression in a collection of patient-derived CAFs grown in FBS or CSS for 7 days (n=18). *NRG1* expression is normalized to *ACTB*.
(E) qRT-PCR analysis of *Nrg1* mRNA expression in 22Pc-CAF grown in FBS, CSS or FBS+Enz for 24 h or 7 days. *Nrg1* expression is normalized to *Actb*.
(F) Western blot analysis of NRG1 expression in 22Pc-CAF (grown in FBS) and in two enzalutamide resistant CWR22Pc tumor derived CAFs (EnzR-CAF #1 and #2, grown in CSS) for 7 days. Cyclophilin B serves as loading control.
(G) qRT-PCR analysis of *Nrg1* mRNA expression in both EnzR-CAFs between CSS and FBS conditions. *Nrg1* expression is normalized to *Actb*.
(H) IGV graphs showing AR binding peaks at *NRG1* and *FKBP5* locus in patient-derived prostate cancer CAFs.

Assays were performed with three biological replicates. ****p<0.0001, ***p<0.001, **p<0.01, *p<0.05, n.s.: not significant, D,G, Student's t-test, B,E: one-way ANOVA compared to FBS/Veh group. Data are represented as mean±SD.

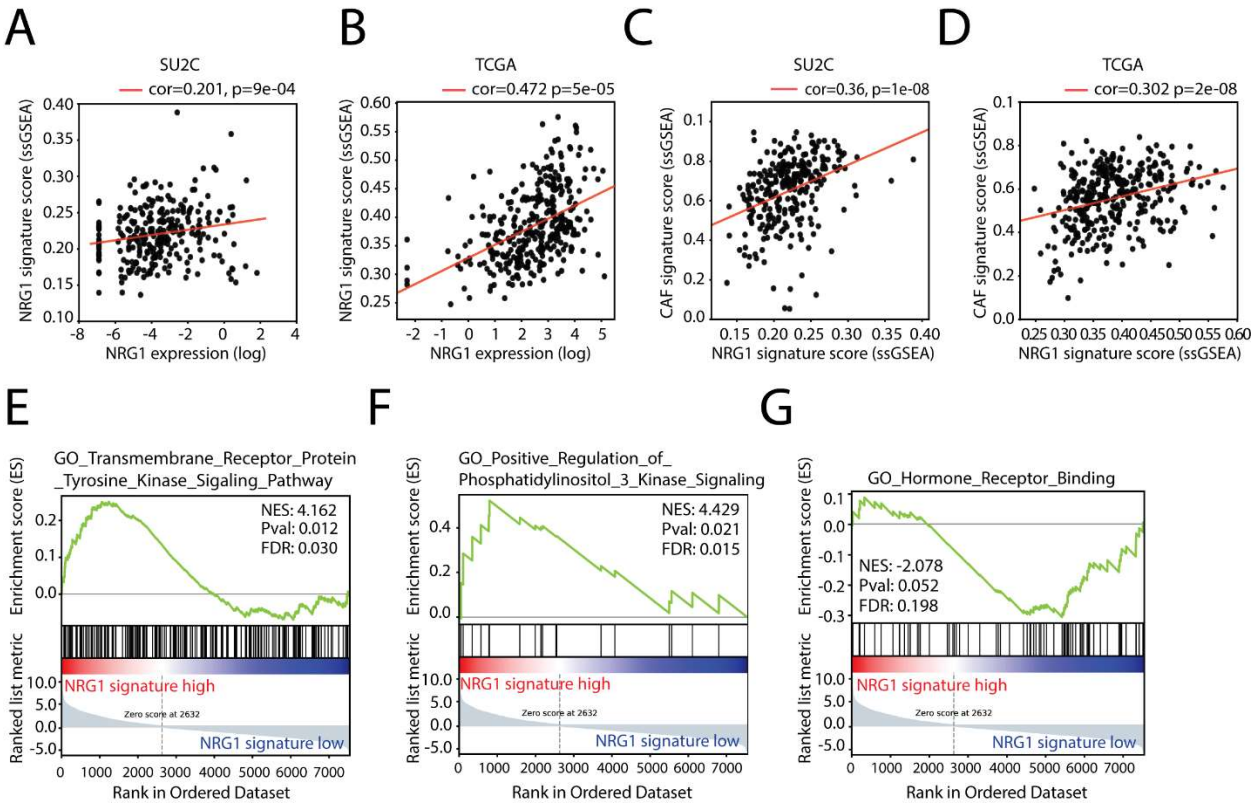

Figure S8 related to Figure 8. NRG1 activity is associated with unfavorable treatment outcome in CRPC patients.

(A) Pearson correlation analysis of NRG1 expression versus NRG1 signature score in SU2C cohort (p value=$9x10^{-4}$).

(B) Pearson correlation analysis of NRG1 expression versus NRG1 signature score in TCGA cohort (p value=$5x10^{-5}$).

(C) Pearson correlation analysis of NRG1 signature score versus CAF signature score (Tyekucheva et al., 2017) in SU2C cohort (p value=$1x10^{-8}$).

(D) Pearson correlation analysis of NRG1 signature score versus CAF signature score (Tyekucheva et al., 2017) in TCGA cohort (p value=$2x10^{-8}$).

(E) GSEA showing Transmembrane Receptor Protein Tyrosine Signaling signature between NRG1 signature -high versus -low groups (median separation).

(F) GSEA showing Positive Regulation of Phosphatidylinostitol-3 Kinase signature between NRG1 signature -high versus -low groups (median separation).

(G) GSEA showing Hormone Receptor Binding signature between NRG1 signature -high versus -low groups (median separation).

Table S4 related to Figure 7. Baseline characteristics in evaluated patients

Characteristic	Neoadjuvant ADT [#] (n = 23)	Hormone intact (n = 20)
Age at diagnosis – years		
Median	58	64
Range	42-70	44-78
Gleason score – n (%)		
7	5 (22)	8 (40)
8	4 (17)	3 (15)
9	13 (57)	7 (35)
10	1 (4)	0 (0)
PSA at diagnosis – ng/mL		
Median	5.8	7.0
Range	1.29-69.9	1.5-20.0
Neoadjuvant treatment – n (%)		
ADT-only	6 (26)	n/a
ADT plus bicalutamide	2 (9)	n/a
ADT plus chemotherapy *	2 (9)	n/a
ADT plus ARSI		n/a
Enzalutamide	4 (17)	n/a
Abiraterone	6 (26)	n/a
Abiraterone plus enzalutamide	3 (13)	n/a
Time on neoadjuvant treatment prior to prostatectomy - days		
Median	166	n/a
Range	92-1038	n/a

[#] Neoadjuvant ADT includes patients who had ADT mean± Abiraterone mean± Enzalutamide prior to radical prostatectomy; IHC: immunohistochemistry; ADT: androgen-deprivation therapy; * 2 patients had docetaxel plus carboplatin concomitant to ADT; n/a: not applicable

Table S5 related to Figure 7. Treatment characteristics and NRG1 expression in patients exposed to neoadjuvant ADT [#]

	Neoadjuvant treatment		IHC for NRG1	
Patient #	Type	Duration (days)	Intensity	Localization
1	ADT	1 dose	Negative	N/A
2	ADT	1 dose	Negative	N/A
3	ADT	1 dose	Negative	N/A
4	ADT, bicalutamide	680	Negative	N/A
5	ADT, chemotherapy	120	Negative	N/A
6	ADT, bicalutamide	277	Negative	N/A
7	ADT, abiraterone	313	Negative	N/A
8	ADT, enzalutamide	363	Negative	N/A
9	ADT, chemotherapy	792	Negative	N/A
10	ADT, abiraterone	1038	Negative	N/A
11	ADT, abiraterone	185	Negative	N/A
12	ADT	1 dose	Negative	N/A
13	ADT	1 dose	Weak	Stroma, Focal
14	ADT	1 dose	Weak	Stroma, Focal
15	ADT, enzalutamide	117	Negative	N/A
16	ADT, abiraterone	325	Negative	N/A
17	ADT, abiraterone	111	Negative	N/A
18	ADT, abiraterone	124	Negative	N/A
19	ADT, abiraterone, enzalutamide	171	Negative	N/A
20	ADT, abiraterone, enzalutamide	166	Negative	N/A
21	ADT, Enzalutamide	167	Positive	Stroma
22	ADT, Enzalutamide	225	Positive	Tumor
23	ADT, abiraterone, enzalutamide	113	Positive	Tumor and Stroma

[#] Neoadjuvant ADT includes patients who had ADT mean± Abiraterone mean± Enzalutamide prior to radical prostatectomy; ADT: androgen deprivation therapy; IHC: Immunohistochemistry

Table S6 related to Figure 7. Characteristics of NRG1 expression in patients exposed to neoadjuvant ADT[#]

Intensity – n (%)	Neoadjuvant ADT [#]	Hormone intact
Negative	17 (74)	20 (100)
Equivocal	1 (4)	0 (0)
Weakly positive	2 (9)	0 (0)
Positive	3 (13)	0 (0)
Localization – n (%)		
Negative	17 (74)	n/a
Tumor only	1 (4)	n/a
Stroma only	3 (13)	n/a
Tumor and stroma	1 (4)	n/a

[#] Neoadjuvant ADT includes patients who had ADT mean± Abiraterone mean± Enzalutamide prior to radical prostatectomy

Table S7 related to Figure 7. Comparison of NRG1 expression between neoadjuvant ADT-exposed and hormone intact patients.

Two-way Contingency Table

	Neoadjuvant ADT [#] (n = 23)	Hormone intact (n = 20)	*P* *
NRG1 expression			0.0265
Negative	18 (78)	20 (100)	
Positive	5 (22)	0 (0)	

[#] Neoadjuvant ADT includes patients who had ADT mean± Abiraterone mean± Enzalutamide prior to radical prostatectomy; * Chi-squared test.
$\chi^2 = 4.920$, df = 1, $\chi^2/df = 4.92$, $P(\chi^2 > 4.920) = 0.0265$